(14) Flory, P. J. *Macrmolecules* **1974**, *7*, 381.
(15) Matsuzaki, K.; Uryu, T.; Ishida, A.; Ohki, T.; Takeuchi, M. *J. Polymn. Sci., Part A-1* **1967**, *5*, 2167.
(16) Le Fevre, R. J. W.; Sundaran K. M. S. *J. Chem. Soc.* **1963**, 3188.
(17) Mikhailov, G. P.; Burshtein, L. *L.*; Malinosvskaya, V. P. *Vysokomol. Soedin., Ser. A* **1969**, *11*, 548 (*Polymn. Sci.* USSR (*Engl. Transl.*) **1969**, *11*, 623).
(18) Kotera, A.; Shimomura, K.; Shima, M. *J. Polym. Sci., Part C* **1970**, *30*, 233.
(19) Masegosa, R. M.; Hernández-Fuentes, I.; Ojalvo, E. A.; Saiz, E. *Macromolecules* **1979**, *12*, 862.

Swelling of Model Poly(dimethylsiloxane) Networks

R. W. Brotzman, Jr.,† and B. E. Eichinger*

Department of Chemistry, BG-10, University of Washington, Seattle, Washington 98195.
Received November 2, 1982

ABSTRACT: Thermodynamically measured sorption data for the swelling of three poly(dimethylsiloxane) networks with cyclohexane at 30 °C are reported. The networks are end linked, with the junction functionalities ϕ and primary-chain molecular weights M_c being as follows (ϕ; M_c): (3; 11 300), (4; 11 300), and (4; 18 500). The swelling function $\lambda\mu_{1,el}$ displays a maximum, where λ^3 is the swelling ratio and $\mu_{1,el}$ the elastic contribution to the solvent chemical potential. These data provide quantitative information on the dependence of swelling upon controlled network structure variations. Results are compared with the theory of Flory and Erman.

Introduction

In previous papers of this series[1,2] we have explored the swelling of elastomers in a variety of solvents by the method of Gee, Herbert, and Roberts.[3] These results uniformly show that the swelling function

$$(\lambda/V_1) \ln (a_{1,c}/a_{1,u}) = f(\lambda^2) \quad (1)$$

exhibits a maximum, contrary to the predictions of the Wall–Flory,[4] James–Guth,[5,6] or Mooney–Rivlin[7,8] theories. Here $\lambda^3 = V/V^\circ$ is the isotropic volume dilation, $a_{1,c}$ is the activity of solvent of molar volume V_1 over a swollen cross-linked polymer, and $a_{1,u}$ is the corresponding activity over an un-cross-linked, but otherwise identical, polymer at the same concentration of solvent.

We have further found evidence that the swelling function $f(\lambda^2)$ is dependent upon the nature of the diluent, contrary to the assumption of Flory and Rehner.[4,9] This observation implies that the elastic and mixing free energies are not strictly separable; there is a cross-term that has not yet been encompassed by theory.

Apart from this anomaly, the recently developed theory of Flory and Erman[10,11] succeeds in predicting the maximum in the swelling function found by Gee et al.[3] and by us. It is the only theory known to us that does so. Now, to further test their predictions, we report measurements on a series of end-linked and well-characterized poly(dimethylsiloxane) (PDMS) networks that have been swollen with cyclohexane at 30 °C. The results allow comparisons of (1) functionality dependence (three and four) for fixed-chain molecule weight (11 300 amu) between junctions and of (2) molecular weight dependence (11 300 amu and 18 500 amu) of the chains for fixed functionality (four). The results will be intercompared with stress–strain isotherms for the same samples obtained by Mark and co-workers and with the Flory–Erman theory.

Experimental Section

The PDMS used for this study was kindly supplied by Professor J. E. Mark. Two networks of functionality ϕ (designated EL1 and EL2) were prepared by reacting vinyl-terminated PDMS chains of known molecular weight with siloxane molecules having ϕ (relatively closely spaced) active hydrogens.[12–18] Another network (designated EL3) was prepared by end-linking hydroxyl-terminated PDMS chains of known molecular weight by means of a tetralkoxysilane.[19–26] The network characteristics of these unimodal samples are given in Table I. At equilibrium swelling in cyclohexane at 30 °C the polymer volume fraction in EL1, EL2, and EL3 are respectively 0.219, 0.223, and 0.146. Prior to the equilibrium swelling measurements, each sample was extracted for 6 days in cyclohexane to remove the soluble impurities. The un-cross-linked PDMS and cyclohexane used were described in a previous paper.[1]

Table I
Summary of Network Characteristics[18,19]

sample	M_c[a]	ϕ[b]
EL1	11 300	3
EL2	11 300	4
EL3	18 500	4

[a] Network chain molecular weight. [b] Junction functionality.

The vapor sorption apparatus[27] and experimental technique[1] have been previously described.

Results and Discussion

Integral sorption and activity measurements yield the Flory–Huggins interaction parameter, $\chi(v_2)$, as a smoothed function of the un-cross-linked polymer volume fraction, v_2. Results for the PDMS + cyclohexane system are shown in Figure 1. The solid line is a least-squares fit through our data at high concentrations and Kuwahara's[28] at low concentrations. The equation for the solid line is

$$\chi = 0.433 - 0.11v_2 \quad (2)$$

The representative osmotic results of Kuwahara, Okazawa, and Kaneko[28] at 20 °C that are represented in Figure 1 as circles have not been corrected to 30 °C because the enthalpy of mixing for this system is not large.[1] Our data consist of results from five separate runs[1,2] using different un-cross-linked PDMS samples from the same lot; there is good agreement between the five data sets.

The differences in solvent mass absorbed by the un-cross-linked and cross-linked PDMS at equal solvent activities were converted into Δv, defined as $v_{1,u} - v_{1,c}$, where subscripts u and c refer respectively to un-cross-linked and cross-linked polymer, from specific volumes given previ-

† Current address: Owens-Corning Fiberglas, Granville, OH 43023.

0024-9297/83/2216-1131$01.50/0

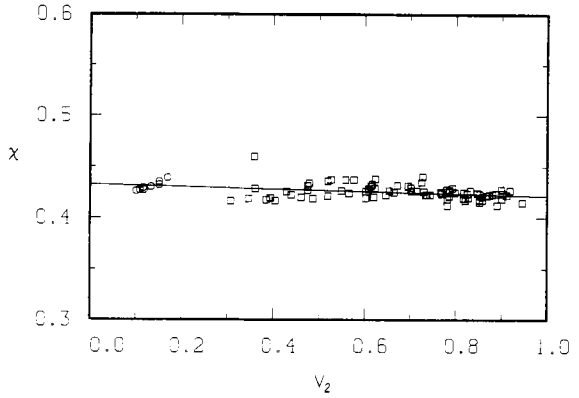

Figure 1. Measured Flory–Huggins interaction parameter, χ, as a function of the volume fraction, v_2, of PDMS in cyclohexane. Squares, vapor sorption data at 30 °C;[1,2] circles, osmotic data of Kuwahara et al.[28] at 20 °C.

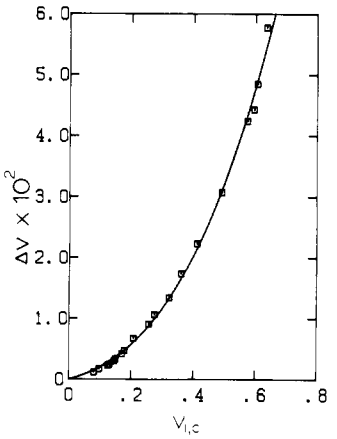

Figure 2. Volume fraction difference vs. volume fraction of cyclohexane in the bulk-cured PDMS (EL1) network at 30 °C.

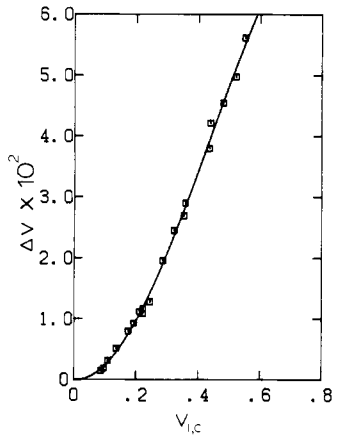

Figure 3. Volume fraction difference vs. volume fraction of cyclohexane in the bulk-cured PDMS (EL2) network at 30 °C.

ously. Experimental differential sorption data for the EL1, EL2, and EL3 + cyclohexane systems are graphed in Figures 2–4. The solid curves in Figures 2–4 are third- or fourth-degree, least-squares polynomials that are constrained to pass through the origin; their equations are respectively

$$\Delta v = 0.0139v_{1,c} + 0.0551v_{1,c}^2 + 0.0921v_{1,c}^3 \quad (3)$$

$$\Delta v = -0.0049v_{1,c} + 0.3000v_{1,c}^2 - 0.1449v_{1,c}^3 - 0.0963v_{1,c}^4 \quad (4)$$

$$\Delta v = -0.0037v_{1,c} + 0.3967v_{1,c}^2 - 0.3954v_{1,c}^3 \quad (5)$$

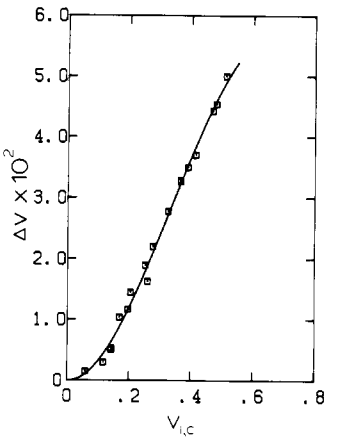

Figure 4. Volume fraction difference vs. volume fraction of cyclohexane in the bulk-cured PDMS (EL3) network at 30 °C.

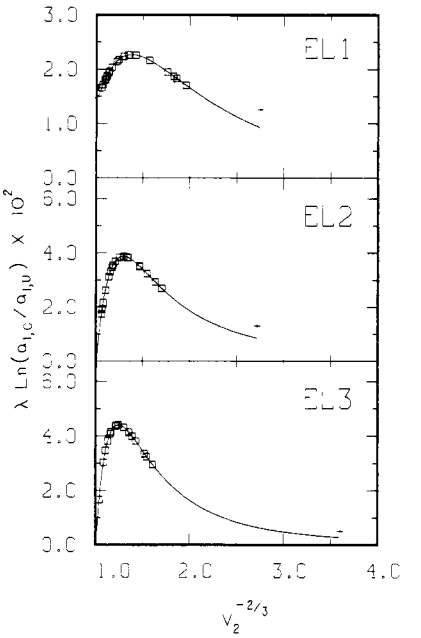

Figure 5. Plot of $\lambda \ln (a_{1,c}/a_{1,u})$ vs. $v_2^{-2/3}$ as a smooth function for PDMS (EL1, EL2, EL3) + cyclohexane at 30 °C; + represents the swelling equilibrium point.

Some of the χ data in the high- and low-concentration range were omitted from the least-squares analysis; they are subject to large errors owing either to the small solvent mass absorbed or to activities approaching unity. At low polymer concentrations the difference between the activity and unity becomes the important quantity, and chemical potentials are subject to large relative errors. However, the errors in the differential and integral mass measurements remained nearly constant throughout this concentration range.

Activity data were obtained by inserting our smoothed functional representations for $\chi(v_2)$ into the mixing contribution to the solvent chemical potential in the form

$$a_1 = v_{1,u} \exp[v_{2,u} + v_{2,u}^2 \chi(v_{2,u})] \quad (6)$$

The procedure to calculate the ratio $a_{1,c}/a_{1,u}$ at equal polymer volume fractions has been previously illustrated.[1]

Derived values of $\lambda \ln (a_{1,c}/a_{1,u})$ are plotted in Figure 5, for the three systems. The crosses represent swelling equilibria. The solid lines in Figure 5 were generated following the above referenced procedure[1] by using values of v_2 ranging from 0.001 to that of swelling equilibrium. The squares represent the concentrations (abscissas) at which data were collected; their ordinates have been

Table II
Summary of Swelling Data

system	max location, $v_2^{-2/3}$	max magnitude, $\times 10^2$	swelling equil	cure type
NR + benzene[3]	1.8	3.7	0.304	bulk-pres[a]
SBR + benzene[27]	1.8	1.5		bulk[b]
SBR + *n*-heptane[27]	1.6	2.0		bulk
PDMS + benzene[27]	1.5	1.2		bulk
PDMS + cyclohexane[1]	1.2	2.3	0.159	soln-radn[c]
PDMS + cyclohexane[2]	1.1	2.6	0.156	bulk-radn[d]
PDMS + benzene[2]	1.3	3.6	0.242	bulk-radn
PDMS (EL1) + cyclohexane	1.3	2.3	0.219	bulk-el[e]
PDMS (EL2) + cyclohexane	1.3	3.9	0.223	bulk-el
PDMS (EL3) + cyclohexane	1.2	4.4	0.146	bulk-el

[a] Bulk cured with sulfur under pressure. [b] Bulk cured with benzophenone sensitizer and ultraviolet radiation. [c] Solution cured (48% polymer volume fraction) with γ radiation. [d] Bulk cured with γ radiation. [e] Bulk cured by end-linking.

smoothed as described above. The swelling equilibrium points were calculated from

$$\ln (a_{1,u}/a_{1,c}) = \ln (1 - v_{2,s}) + v_{2,s} + \chi v_{2,s}^2 \quad (7)$$

where $v_{2,s}$ is the volume fraction of cross-linked polymer at swelling equilibrium, and χ is obtained by interpolation using eq 2. Swelling equilibria data were *not* included in the polynomial fits given in eq 3–5. As can be seen from Figure 5, $\lambda \ln (a_{1,c}/a_{1,u})$ exhibits a maximum when plotted against $v_2^{-2/3}$ for each system. Such maxima have been found in all systems studied to date, both solution and bulk cured. Table II contains a summary of these systems, the location of their maxima, and the network cure type. A comparison between the two chemically characterized PDMS + cyclohexane systems of equal chain molecular weight reveals that the tetrafunctional (EL2) sample displays a sharper maximum of greater magnitude (3.9×10^{-2} vs. 2.3×10^{-2}) than its trifunctional (EL1) counterpart; both maxima occur at approximately the same location ($v_2^{-2/3} = 1.30$ and 1.33, respectively). On comparing the tetrafunctional networks, EL2 and EL3, one finds that the maximum is larger (3.9×10^{-2} vs. 4.4×10^{-2}) and shifted to lower dilutions ($v_2^{-2/3} = 1.30$ vs. $v_2^{-2/3} = 1.24$) as the network chain molecular weight increases from 11 300 (EL2) to 18 500 (EL3).

Analysis Using Flory Theory

The recently reformulated elasticity theory of Flory and Erman[10,11] gives results to be recounted here. For swelling, the elastic contribution to the solvent chemical potential is

$$\lambda \ln (a_{1,c}/a_{1,u}) = (\xi V_1/V^\circ)[1 + (\mu_j/\xi)K(\lambda^2)] \quad (8)$$

where μ_j is the number of junctions, ξ is the cycle rank of the network, V_1 is the diluent molar volume, V° is the network volume in the reference state, and

$$K(\lambda^2) = B[\dot{B}(1 + B)^{-1} + g(\dot{g}B + g\dot{B})(1 + gB)^{-1}] \quad (9a)$$

$$B = (\lambda - 1)[1 + \lambda - \zeta\lambda^2](1 + g)^{-2} \quad (9b)$$

$$g = \lambda^2[\kappa^{-1} + \zeta(\lambda - 1)] \quad (9c)$$

$$\dot{B} = B[(\lambda - 1)^{-1}(1/2\lambda) + (1 + \lambda - \zeta\lambda^2)^{-1}(1/2\lambda - \zeta) - 2\dot{g}(1 + g)^{-1}] \quad (9d)$$

$$\dot{g} = \kappa^{-1} - \zeta(1 - 3\lambda/2) \quad (9e)$$

$$\kappa = \sigma_0/\rho = \langle(\Delta R)^2\rangle/\langle(\Delta x_1)^2\rangle \quad (9f)$$

$$\zeta = \rho/\sigma_2 = \langle(\Delta x_2)^2\rangle/\langle(\Delta R)^2\rangle \quad (9g)$$

where Δx_1 represents the displacement from the center of action of an entanglement constraint and Δx_2 is an additional displacement introduced by deviations from the perfectly affine state due to structural irregularities. The parameters κ and ζ measure respectively the severity of constraints exerted by neighboring chains and the magnitude of fluctuations due to irregularities relative to those of the phantom network.

For uniaxial deformation, the reduced force is defined by

$$[f^*] = f^*(V/V^\circ)^{-1/3}(\alpha - \alpha^{-2})^{-1} \quad (10)$$

where f^* is the tensile force per unit area measured in the reference state V°, V is the system volume at measurement, and α is the extension ratio relative to the isotropic sample length at the same volume V. From theory,[10,29]

$$[f^*] = [f^*_{ph}](1 + f_c/f_{ph}) \quad (11)$$

where f_{ph} is the force exerted by an equivalent phantom network at the same elongation, f_c is the contribution to the force from constraints on junction fluctuations, and $[f^*_{ph}]$ is the reduced force in the limit of high extension. The reduced force for the equivalent phantom network is[29,30]

$$[f^*_{ph}] = (\xi kT/V^\circ) \quad (12)$$

For uniaxial deformations the principal extensions are

$$\lambda_1 = \alpha(V/V^\circ)^{1/3}$$

$$\lambda_2 = \lambda_3 = \alpha^{-1/2}(V/V^\circ)^{1/3} \quad (13)$$

and the ratio f_c/f_{ph} is given by

$$(f_c/f_{ph}) = (\mu_j/\xi)[\alpha K(\lambda_1^2) - \alpha^2 K(\lambda_2^2)](\alpha - \alpha^{-2})^{-1} \quad (14)$$

For a perfect network free of defects the cycle rank (ξ), number of junctions (μ_j), and the network functionality (ϕ) are related by

$$\xi = \mu_j(\phi - 2)/2 \quad (15)$$

Flory has proposed that κ is related to $[f^*_{ph}]$ by[11]

$$\kappa = I[f^*_{ph}]^{-1/2}[2/(\phi - 2)] \quad (16)$$

where I is a universal interpenetration parameter. For networks of a given kind, κ is predicted to vary inversely as the square root of the reduced force in the phantom network limit.

Mark and co-workers[18,19] have determined both the stress–strain isotherms in elongation at 25 °C and the equilibrium swelling in benzene at room temperature for samples EL1, EL2, and EL3. Their results are compared with theoretical calculations in Figure 6 for $\zeta = 0.0$. The solid curves in Figure 6 were generated from eq 16; the dashed curve was generated for arbitrary κ and $[f^*_{ph}]$ to

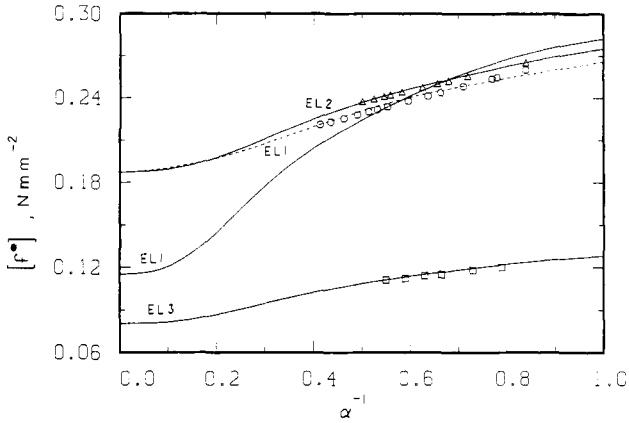

Figure 6. Results of Mark and co-workers[18,19] for end-linked PDMS networks. Circles, EL1; triangles, EL2; squares, EL3. Values of the parameters used for theoretical calculations are given in Table III.

Table III
Summary of Theoretical Parameters

figure	sample	$[f^*_{ph}]$, N/mm²	κ	ζ	μ_j/ξ
6	EL1	0.115	11.76	0.0	2
6	EL2	0.187	4.52	0.0	1
6	EL3	0.080	6.90	0.0	1
6 (dash)	EL1	0.187	1.70	0.0	2
8	EL1	0.160	10.36	0.2	2
8	EL2	0.210	4.52	0.2	1
8	EL3	0.095	6.72	0.2	1

give a best fit to the data. Table III is a summary of the pertinent theoretical parameters. There is a close agreement between theory and experiment for tetrafunctional EL2 and EL3; however, the arbitrarily generated dashed curve more closely fits EL1 data. For tetrafunctional networks, eq 16 reduces the Flory–Erman theory to a three-parameter theory. However, all four parameters are required to describe trifunctional behavior.

How well do the stress–strain theoretical fits predict swelling behavior? Figure 7 illustrates the swelling behavior predicted from the stress–strain fits with $\zeta = 0.0$; agreement between experiment and theory is poor for this choice of ζ. If ζ is set to 0.2, the fit to the swelling data is improved at the expense of a somewhat poorer fit of the stress–strain data (Figures 8 and 9). The swelling functions depicted in Figure 9 more closely agree with experimental data, but the corresponding fit to stress–strain isotherms using these parameters is poorer. The stress–strain data can be fitted at the expense of poor agreement with swelling data, and vice versa.

The above arguments demonstrate that a single set of theroetical parameters cannot describe both swelling and stress–strain behavior. However, theory does predict that for EL2 and EL1 the maximum in $\lambda \ln (a_{1,c}/a_{1,u})$ should occur at about the same value of $v_2^{-2/3}$ and that its magnitude will be greater for EL2 than for EL1; this is experimentally observed. The differences between the parameters required to fit the data for tri- and tetrafunctional networks cast doubt upon the form of the universal interpenetration parameter given in eq 16.

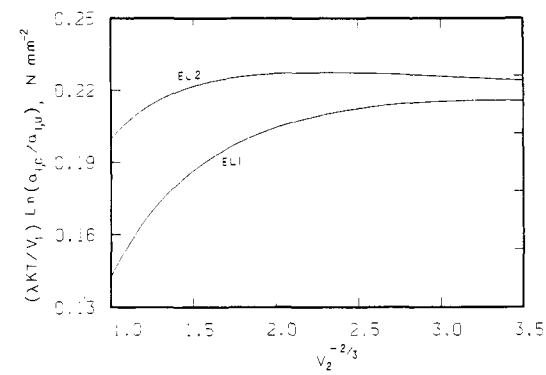

Figure 7. Theoretical dependence of $(kT/V_1)\lambda \ln (a_{1,c}/a_{1,u})$ upon $v_2^{-2/3}$ as given by eq 8 for EL1 and EL2. Theoretical parameters are given in Table III (solid curves in Figure 6; $\zeta = 0$).

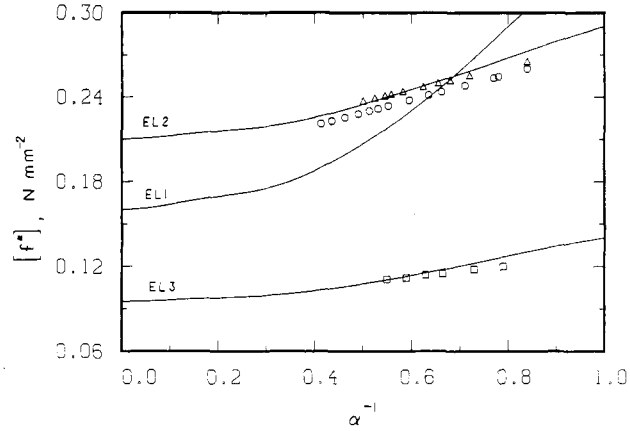

Figure 8. Results of Mark and co-workers[18,19] for end-linked PDMS networks. Circles, EL1; triangles, EL2; squares, EL3. Values of the parameters used for theoretical calculations are given in Table III.

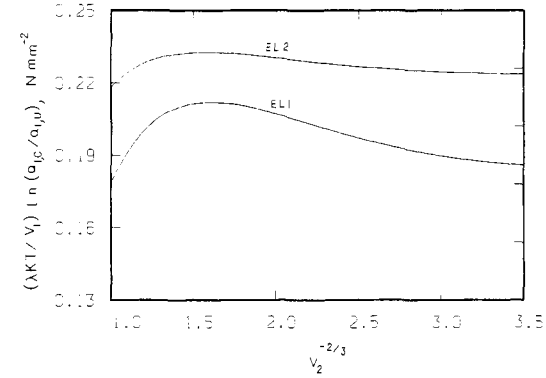

Figure 9. Theoretical dependence of $(kT/V_1)\lambda \ln (a_{1,c}/a_{1,u})$ upon $v_2^{-2/3}$ as given by eq 8 for EL1 and EL2. Theoretical parameters are given in Table III (Figure 8; $\zeta = 0.2$).

Cycle-rank densities can be calculated from swelling equilibrium results from the equation

$$\xi/V^\circ N_A = -(\lambda/V_1)[1 + (\mu_j/\xi)K(\lambda^2)]^{-1}[\ln (1 - v_2) + v_2 + \chi v_2^2] \quad (17)$$

Table IV
Cycle-Rank Densities Calculated from Swelling Equilibrium in Benzene (B) and Cyclohexane (C)

	κ	ζ	μ_j/ξ	$V_{2,s}{}^{B}$[14,15]	$(\xi/V^\circ)^B \times 10^4$, mol/cm³	$V_{2,s}{}^{C}$	$(\xi/V^\circ)^C \times 10^4$, mol/cm³	$d(\phi - 2)/\phi M_c \times 10^4$, mol/cm³
EL1	10.36	0.2	2	0.312	0.947	0.219	1.361	0.283
EL2	4.52	0.2	1	0.330	1.149	0.223	1.329	0.425
EL3	6.72	0.2	1	0.213	0.381	0.146	0.568	0.262

which is derived by equating the elastic and mixing contributions to the solvent chemical potential at swelling equilibrium. The results for the swelling of the three networks in cyclohexane and in benzene[18,19] are given in Table IV. Our data for the interaction parameter χ for PDMS with cyclohexane and with benzene[2] were used in this analysis.

The cycle-rank density can also be estimated from the chain molecular weight by

$$\xi/V^\circ N_A = d(\phi - 2)/\phi M_c \tag{18}$$

where d is the density and M_c is the chain molecular weight (both d and M_c were given by Mark[18,19]). The benzene and cyclohexane cycle-rank densities differ by 30%, 14%, and 33% for EL1, EL2, and EL3, respectively. These differences are much larger than expected from experimental error. Even greater differences are seen between values of the cycle-rank densities calculated with the use of eq 18.

From eq 8, the swelling function maximum is nearly proportional to the respective cycle-rank density. Experimentally the maximum for EL3 is greater than that of EL2 (4.4×10^{-2} vs. 3.9×10^{-2}); data in Table IV would lead one to expect the opposite behavior. Can the parameters κ and ζ be varied in such a way as to theoretically justify the experimental results?

An increase in κ or a decrease in ζ would cause the maximum to increase.[2] For Gaussian chains the fluctuations in the chain vectors are approximately related to the magnitude of the chain vectors according to[30,32]

$$\langle(\Delta R)^2\rangle = (2/\phi)\langle r^2\rangle_0 \tag{19}$$

Thus from eq 8, 9f, and 9g, these are the directions in which κ and ζ would change (for a given functionality) if the network chain lengths were to increase. But as seen from Figure 7 in ref 2, the resultant increase in the maximum would be at most 10–20%. This increase is not sufficient to rectify the discrepancy between theory and experiment.

One should not attach too much importance to the agreement or disagreement between the Flory–Erman theory and these experiments. So long as the specific solvent effect reported in the previous paper remains incomprehensible, there is a corresponding uncertainty in the significance of the values assigned to the theoretical parameters chosen to fit the data. For the present, we believe that the Flory–Erman theory applies to a hypothetical swelling process, where the specific solvent effect is nil.

Thermodynamic Swelling Cycle

Some insight into the source of the specific solvent effect may be gleaned from the following thermodynamic cycle:[33]

$$\begin{array}{ccc} \mathrm{E}(0) + n\mathrm{S} & \xrightarrow{\Delta G} & \mathrm{E}(v_1) \\ \Big\downarrow -\Delta G_x(0) & & \Big\uparrow \Delta G_x(v_1) \\ \mathrm{L}(0) + n\mathrm{S} & \xrightarrow{\Delta G_m} & \mathrm{L}(v_1) \end{array} \tag{20}$$

Here E, L, and S denote elastomer, linear chains, and solvent, respectively; when the elastomer imbibes n moles of solvent it swells so that the volume fraction of solvent is v_1. The free energy change accompanying this process is ΔG, whereas ΔG_m is the corresponding free energy change when linear chains are dissolved in the same quantity of solvent to produce a solution with the same composition. The cross-linking of $\mathrm{L}(v_1)$ to form $\mathrm{E}(v_1)$, either in bulk ($v_1 = 0$) or in solution ($v_1 \neq 0$), entails the free energy change $\Delta G_x(v_1)$.

One of these cross-linking reactions is irreversible. If the elastomer being considered was cured in the dry state, then $\mathrm{L}(v_1) \rightarrow \mathrm{E}(v_1)$ is *irreversible* because the set of networks formed on curing in solution in this step of the cycle must be identical, in all respects consistent with ensemble averaging, with the networks cured in the bulk. This is impossible because network topology, or connectivity, depends upon the chain density at the time of cure. Conversely, if the elastomer was cured in solution, so that $\mathrm{L}(v_1) \rightarrow \mathrm{E}(v_1)$ is reversible, then $\mathrm{L}(0) \rightarrow \mathrm{E}(0)$ is irreversible because the array of connected networks produced by a reversible reaction in the dry state will not have identically the same statistical weights in the ensemble as do those that were produced in the solution cure.

The essence of the swelling experiments reported here and in previous papers is that they give directly (upon integrating the chemical potential) the quantity

$$\Delta G_{el} = \Delta G - \Delta G_m = \Delta G_x(v_1) - \Delta G_x(0) \tag{21}$$

The consistent experimental observation that $\Delta G_{el} \neq 0$ for all polymer–solvent pairs studied is proof that $\Delta G_x(v_1) \neq \Delta G_x(0)$, as asserted in the preceding paragraph.

These considerations cast new light on swelling experiments: We are being told something about network connectivity. As Flory and Rehner first showed, the primary information to be gotten from swelling equilibrium is the cross-link density; in the more recent theoretical developments the cycle rank of the network replaces the cross-link density. Perhaps a more comprehensive theory of the solvent dependence of swelling will provide the means to obtain other characteristics of network structure.

Conclusions

This investigation allows comparison of the elastic components of the solvent chemical potential for chemically characterized PDMS + cyclohexane systems. A unimodal tetrafunctional model network displays a sharper maximum of greater magnitude than its trifunctional counterpart; both maxima occur at approximately the same swelling ratio. For tetrafunctional model networks, the maximum is larger and shifts to lower dilution as network chain lengths increase.

The Flory–Erman theory has been compared with swelling and stress–strain (elongation) isotherms for the three networks. In each case, a single set of theoretical parameters does not accurately describe both the swelling and stress–strain behavior. Nonetheless, the theory shows general qualitative agreement with experiment.

It is now clear that the elastic and mixing free energies are not separable because of the observed specific solvent effects as demonstrated by earlier experiments.[2,27] The source of this effect is traceable to the influence of solvent on network topology at the time of cure.

Acknowledgment. We are grateful to Professor J. E. Mark for his generous donation of samples. This work was supported, in part, by Department of Energy Contract DE-AT06-81ER10912. R.W.B. benefited from a Chevron summer fellowship sponsored by Standard Oil of California.

Registry No. Cyclohexane, 110-82-7.

References and Notes

(1) Brotzman, R. W.; Eichinger, B. E. *Macromolecules* **1981**, *14*, 1445.
(2) Brotzman, R. W.; Eichinger, B. E. *Macromolecules* **1982**, *15*, 531.
(3) Gee, G.; Herbert, J. B. M.; Roberts, R. C. *Polymer* **1965**, *6*, 541.

(4) Flory, P. J. J. Chem. Phys. 1953, 18, 108, 112.
(5) James, H. M.; Guth, E. J. Chem. Phys. 1943, 11, 455; 1947, 15, 699; 1953, 21, 1039; J. Polym. Sci. 1949, 4, 153.
(6) James, H. M. J. Chem. Phys. 1947, 15, 651.
(7) Mooney, M. J. Appl. Phys. 1940, 11, 582.
(8) Rivlin, R. S. Philos. Trans. R. Soc. London, Ser. A 1948, no. 240, 459; 1948, no. 241, 379; 1949, no. 242, 173.
(9) Flory, P. J.; Rehner, J., Jr. J. Chem. Phys. 1943, 11, 521. James, H. M.; Guth, E. Ibid. 1943, 11, 455.
(10) Flory, P. J.; Erman, B. Macromolecules 1982, 15, 800.
(11) Erman, B.; Flory, P. J. Macromolecules 1982, 15, 806.
(12) Valles, E. M.; Macosko, C. W. Rubber Chem. Technol. 1976, 49, 1232.
(13) Valles, E. M.; Macosko, C. W. In "Chemistry and Properties of Cross-Linked Polymers"; Labana, S. S., Ed.; Academic Press: New York, 1977.
(14) Valles, E. M.; Macosko, C. W. Macromolecules 1979, 12, 673.
(15) Falender, J. R.; Yeh, G. S. Y.; Mark, J. E. J. Chem. Phys. 1979, 70, 5324.
(16) Falender, J. R.; Yeh, G. S. Y.; Mark, J. E. J. Am. Chem. Soc. 1979, 101, 7353.
(17) Falender, J. R.; Yeh, G. S. Y.; Mark, J. E. Macromolecules 1979, 12, 1207.
(18) Llorente, M. A.; Mark, J. E. Macromolecules 1980, 13, 681.
(19) Mark, J. E.; Sullivan, J. L. J. Chem. Phys. 1977, 66, 1006.
(20) Sullivan, J. L.; Mark, J. E.; Hampton, P. G., Jr.; Cohen, R. E. J. Chem. Phys. 1978, 68, 2010.
(21) Mark, J. E.; Rahalkar, R. R.; Sullivan, J. L. J. Chem. Phys. 1979, 70, 1794.
(22) Llorente, M. A.; Mark, J. E. J. Chem. Phys. 1979, 71, 682.
(23) Mark, J. E. Makromol. Chem., Suppl. 1979, 2, 180, 87.
(24) Mark, J. E.; Llorente, M. A. J. Am. Chem. Soc. 1980, 102, 632.
(25) Llorente, M. A.; Mark, J. E. J. Polym. Sci., Polym. Phys. Ed. 1980, 18, 181.
(26) Andrady, A. L.; Llorente, M. A.; Mark, J. E. J. Chem. Phys. 1980, 72, 2282.
(27) Yen, L. Y.; Eichinger, B. E. J. Polym. Sci., Polym. Phys. Ed. 1978, 16, 117, 121.
(28) Kuwahara, N.; Okazawa, T.; Kaneko, M. J. Polym. Sci., Part C 1968, no. 23, 543.
(29) Flory, P. J. Polym. Prepr., Am. Chem. Soc., Div. Polym. Chem. 1981, 22 (2), 150.
(30) Flory, P. J. Proc. R. Soc. London, Ser. A 1976, 351, 351.
(31) Flory, P. J. J. Chem. Phys. 1977, 66, 5720.
(32) Eichinger, B. E. Macromolecules 1972, 5, 496.
(33) Flory, P. J. J. Chem. Phys. 1950, 18, 108.

Preferential Solvation in Polymer–Monomer–Solvent Systems and Its Potential Effect on the Kinetics of Polymerization

Pavel Kratochvil,* Dagmar Straková, Jaroslav Stejskal, and Zdeněk Tuzar

Institute of Macromolecular Chemistry, Czechoslovak Academy of Sciences, 162 06 Prague 6, Czechoslovakia. *Received September 1, 1982*

ABSTRACT: A model of the effect of preferential solvation of the polymer on the kinetics of polymerization in ternary polymer–monomer–solvent systems has been suggested. The extent of preferential solvation was measured by the light scattering and refractive index increment methods for a number of typical systems. In most cases, preferential solvation can be expected to change the rate of polymerization by a few percent. At low monomer concentrations, larger effects are more likely to occur than at high monomer concentrations.

One of the potential causes of frequently observed deviations of the real polymerization course in the presence of an inert solvent or solvent mixture from the classical kinetic scheme is seen in the preferential solvation of the propagating polymer chain by either monomer, or solvent, or some component of the solvent mixture.[1-3] It is known that, due to the preferential binding of some components of a multicomponent solvent by the polymer, in dilute polymer solutions the solvent composition within the domains of polymer molecules generally differs from its composition in volume elements of solution that remain unaffected by the force effects of segments of the polymer molecule.[4-6] Preferential binding of the monomer by the polymer may accelerate the polymerization compared with the rate corresponding to an average, analytically detectable monomer concentration in the system, and, vice versa, preferential sorption of the solvent on the polymer may slow down the polymerization. Similar reasonings hold for copolymerizations even in the absence of solvent; preferential sorption may also be one of the causes underlying the dependence of the monomer reactivity ratios on the nature of the solvent observed in some systems.

While the qualitative image of the effect is clear, its actual influence has so far been demonstrated rather by indirect experimental evidence, and a quantitative correlation between the magnitude of preferential solvation and effects upon the polymerization kinetics due to it is still lacking.

The influence of preferential sorption on the rate of propagation of a polymer chain has been analyzed theoretically by Kozlov and Enikolopyan.[7] They assumed that the thermodynamic behavior of the polymer solution in a monomer–solvent mixture is controlled by Flory–Huggins theory with binary interaction parameters and came to the conclusion that preferential sorption of the monomer or solvent may change the rate of polymerization up to a few tens of per cents.

Locatelli and Riess[8-11] investigated the effect of preferential sorption in the formation of graft copolymers of the ABS (acrylonitrile–butadiene–styrene) type in great detail. The finding that styrene–acrylonitrile chains grafted on polybutadiene have a higher content of styrene constitutional units than ungrafted molecules of a statistical copolymer of styrene and acrylonitrile formed in parallel with the grafts is consistent with a view that in a solution of polybutadiene in a styrene–acrylonitrile mixture polybutadiene is preferentially solvated with styrene. It seems that, in this reaction, the inititator is also nonuniformly distributed in the system owing to preferential sorption,[10] which affects the polymerization kinetics.

The extent of preferential sorption in a number of ternary polymer–monomer–solvent systems related to the formation of statistical copolymers of styrene and acrylonitrile in a toluene or dimethylformamide solution was measured by Pichot et al.,[12] who also compared their results with some phenomena observed in the copolymerization.

The dependence of the rate of polymerization of methyl methacrylate on the monomer concentration in a solution with cyclohexanone, preferentially bound by the polymer,[13]

0024-9297/83/2216-1136$01.50/0